ՀՀ ԳԱԱ Վ. Համբարձումյանի անվան Բյուրականի աստղադիտարան

Անահիտ Լյովայի Սամսոնյան

«Փոշով հարուստ աստղառաջացման բռնկումով գալակտիկաների և ակտիվ գալակտիկական միջուկների ուսումնասիրությունը ենթակարմիր [CII] 158 մկմ առաքման գծի միջոցով»

Ա.03.02 - «Աստղաֆիզիկա, ռադիոաստղագիտություն» մասնագիտությամբ ֆիզիկամաթեմատիկական գիտությունների թեկնածուի գիտական աստիճանի հայցման ատենախոսության

ՍԵՂՄԱԳԻՐ

Բյուրական – 2025

NAS RA Byurakan Astrophysical Observatory after V. Ambartsumian

Anahit L. Samsonyan

“Investigation of the dusty Starburst galaxies and Active Galactic Nuclei through the infrared [CII] 158 μm emission line”

Thesis for the degree of candidate in physical and mathematical sciences
Specialty 01.03.02 – “Astrophysics and Radioastronomy”

SYNOPSIS

Byurakan – 2025

Ատենախոսության թեման հաստատվել է ՀՀ ԳԱԱ Վ. Համբարձումյանի անվան Բյուրականի աստղադիտարանի գիտական խորհրդում:
Գիտական ղեկավար՝

Ֆ.մ.գ.դ. Արարատ Եղիկյան

Պաշտոնական ընդդիմախոսներ՝

Ֆ.մ.գ.դ. Գևորգ Հաջյան

Ֆ.մ.գ.թ. Արեգ Միքայելյան

Առաջատար կազմակերպություն՝

Վրացական ազգային Աբասթումանի աստղադիտարան

Պաշտպանությունը կայանալու է 2025 թ. փետրվարի 27-ին ժամը 14:00-ին, ՀՀ ԳԱԱ Վ. Համբարձումյանի անվան Բյուրականի աստղադիտարանում, «Աստղաֆիզիկա, ռադիոաստղագիտություն» № 048 մասնագիտական խորհրդում:
Ատենախոսությանը կարելի է ծանոթանալ ՀՀ ԳԱԱ Վ. Համբարձումյանի անվան Բյուրականի աստղադիտարանի գրադարանում:
Սեղմագիրը առաքված է 2025 թ. հունվարի 24-ին:
Մասնագիտական խորհրդի գիտական քարտուղար՝ Ֆ.մ.գ.թ. Հայկ Աբրահամյան

The thesis theme is approved by the scientific council of the NAS RA Byurakan Astrophysical Observatory after V. Ambartsumian
Scientific advisor:

Doctor of Phys. Math. Sciences Ararat Yeghikyan

Official opponents:

Doctor of Phys. Math. Sciences Gevorg Hajyan

Candidate of Phys. Math. Sciences Areg Mickaelian

Leading Organization:

Georgian National Astrophysical Observatory of Abastumani

The defense of the thesis will take place at 14:00 on February 27 on the session of the Special Council “Astronomy, radioastronomy” № 048 of the NAS RA Byurakan Astrophysical Observatory after V. Ambartsumian.
The thesis is available in the library of NAS RA Byurakan Astrophysical Observatory after V. A. Ambartsumian.
The synopsis is distributed on 24 January 2025.
Scientific secretary of the Special Council Candidate of Phys. Math. Sciences Hayk Abrahamyan

General description of the thesis

Relevance of the topic

Understanding the initial formation of galaxies depends on discovering sources obscured by dust and tracing these sources to their earliest epoch in the universe. The extreme luminosity of dusty, local sources was originally revealed by the ultraluminous infrared galaxies (ULIRGs), whose luminosity arises from infrared emission by dust, and this dust often obscures the primary optical sources of luminosity. That such galaxies are important in the early universe was demonstrated by source modeling which indicated that the infrared dust emission from galaxies dominates the cosmic background luminosity.

Surveys in the submillimeter were the first to discover individual, optically obscured, dusty sources at redshifts $z >= 2$. A variety of observing programs using spectra from the Spitzer Infrared Spectrometer (IRS) subsequently found luminous ULIRGs to redshifts $z\sim3$. This Spitzer-discovered population of high-redshift ULIRGs has large infrared-to-optical flux ratios [fv (24 μm) > 1 mJy and R > 24] attributed to heavy extinction by dust and has been labeled "dust obscured galaxies" (DOGs). Some DOGs are powered primarily by starbursts and some by active galactic nuclei (AGNs), and the DOGs are similar to the population of submillimeter galaxies in overall spectral energy distributions (SEDs), redshifts, and Luminosities.

To discover and understand dusty galaxies at even higher redshifts than the DOGs known so far, the atomic line emission of [CII] 158 μm is the single most important spectroscopic feature because it is the strongest far-infrared line. Consequently, this line will provide the best opportunity for redshift determinations and source diagnostics using submillimeter and millimeter spectroscopic observations. Already, [CII] has been detected at redshift exceeding 8 and shown to be strong in starbursts with $1 < z < 2.5$. The [CII] line should be a diagnostic of star formation because it is primarily associated with the photodissociation region (PDR) relating to starbursts (SBs).

In many high-redshift sources, especially dust-obscured sources, the [CII] feature is the only diagnostic atomic emission line that can be observed. This makes it vital to optimize this line for learning about intrinsic source properties. Not only line luminosities, but also accurate line profiles, are observed.

A great amount of diagnostic information concerning the observable differences between dusty, obscured sources powered by active galactic nuclei (AGNs) and those powered by rapid star formation ("starbursts") has been acquired via the mid-infrared spectroscopy of the Infrared Spectrograph (IRS) on the Spitzer Space Telescope. Classifications of AGN and Starburst sources have been developed using both the strength of polycyclic aromatic

hydrocarbon (PAH) features in low-resolution spectra and various emission line ratios in high-resolution spectra.

These findings underscore the critical role of far-infrared diagnostics, particularly the [CII] 158 μm emission line, in unraveling the complexities of galaxy evolution. The integration of mid-infrared spectroscopic tools, submillimeter observations, and advanced classifications has significantly advanced our ability to differentiate between AGN-driven and starburst-driven processes in dusty, high-redshift galaxies. By leveraging the [CII] line as a robust tracer of star formation and interstellar medium properties, this research provides a foundation for probing the earliest stages of galaxy formation, bridging observational gaps, and refining models of cosmic evolution. The capability to study both the physical conditions and kinematics of these distant galaxies sets a path for future explorations, further enabling the discovery of hidden populations of galaxies in the early universe.

The aim of the thesis

The primary aim of this thesis is to investigate the physical properties and processes occurring in dusty starburst galaxies and active galactic nuclei (AGN) using the [CII] 158 μm emission line as a diagnostic tool. By exploring the correlation between [CII] luminosities, star formation rates (SFRs), and mid-infrared emission features, the research aims to:

1. Enhance the understanding of the interplay between star formation and AGN activity in galaxies.
2. Refine the use of the [CII] 158 μm line as a robust tracer for SFR, particularly in dusty environments.
3. Provide insights into the evolutionary stages of galaxies, focusing on high-redshift systems obscured by dust.

This work contributes to the broader effort of understanding the role of infrared emission lines in tracing the processes governing galaxy formation and evolution across cosmic time.

Scientific novelty

The scientific novelty of this research lies in several key areas:

1. *Refinement of [CII] as a Star Formation Tracer:*

   This study provides a detailed calibration of the [CII] 158 μm line to measure star formation rates, particularly for dusty galaxies where optical tracers fail. It examines

the relationship between [CII] luminosities and other star formation indicators across a wide range of galaxy types: Active Galactic Nuclei (AGN), Composite and Sturbusrt (SB) galaxies.

2. *Insights into the [CII] Deficit:*

The thesis discusses possible reasons behind the [CII] deficit, a phenomenon where [CII] emission weakens in luminous systems. The [CII] "deficit," or a smaller ratio of $L([CII])/L_{ir}$ with increasing L_{ir}, is shown to arise because L_{ir} of the most luminous sources arises primarily from an AGN so that L([CII]) from the starburst component is small in comparison.

3. *High-Redshift Focus:*

While focused on galaxies in the near universe, this research establishes relationships between [CII] luminosities and star formation indicators, offering a foundation to apply these diagnostics to galaxies during the epoch of reionization ($z > 6$) in future studies.

4. *Integration of Multi-Wavelength Data:*

Having opportunity to classify the galaxies using PAH emission features on mid-infrared spectra and comparing [CII] measurements with mid-infrared fine-structure lines allows a comprehensive understanding of the physical conditions in star-forming and AGN-dominated regions.

Practical importance

The practical importance of this thesis is rooted in its potential applications for observational astronomy and galaxy evolution studies. The results greatly contribute to the development of infrared astronomy by providing methods to estimate the rate of star formation and detect the activity of AGN in dusty, distant galaxies. These insights are important for understanding the evolution of the early Universe and for developing future observational programs for telescopes such as ALMA. The thesis also contributes to the theory of a unified model of AGN, linking spectral properties to physical processes in Active Galactic Nuclei.

Basic results to be defended

1. *Classification of 379 galaxies:*

   We classify 379 galaxies as AGN, Composite or Starburst observed both with Spitzer Space Telescope and Hershcel Space Observatory. Results for [CII] and neon lines are compared by locating the PACS observing spaxel that most closely

corresponds to the position of the IRS slit. Intrinsic line profile widths are determined by applying empirically measured instrumental widths from observed planetary nebulae or HII regions. All [CII] and neon line profiles, together with overlays of PACS spaxels compared to IRS slits, are illustrated in the CASSIS spectral atlas (*http://cassis.sirtf.com/herschel*).

2. *Star formation rate (SFR) calibration using [CII] 158 μm emission line:*
   The calibrated relationships between [CII] luminosities and SFRs enable more accurate interpretation of data from infrared and submillimeter observatories. The work provides a stable calibration of the star formation rate, particularly in dusty environments where the known optical lines measuring the star formation rate are absorbed. The thesis shows that the luminosity of [CII] depends somewhat on the star formation rate as follows: $\log(SFR) = \log L([CII]) - 7.0 \pm 0.2$ for SFR in $M_\odot$ s yr^{-1} and L([CII]) in $L_\odot$s. This is a breakthrough result, especially for the study of distant galaxies at high redshift, where other indices are unavailable.
3. *6.2 μm PAH feature as a Classification Criterion:*
   The thesis establishes the 6.2 μm PAH feature as a crucial tool for classifying sources, distinguishing AGN-dominated galaxies from starburst-dominated systems. We have adopted the criteria that AGNs have EW (6.2 μm) < 0.1 μm, Composite sources have intermediate 0.1 μm < EW (6.2 μm) < 0.4 μm, and starbursts have EW (6.2 μm) > 0.4 μm. This classification criterion provides a robust method for identifying the primary drivers of galactic emission.
4. *[CII] 158 μm line as Starburst indicator:*
   Detailed study of [CII] 158 μm line profiles and the comparison with PAH 11.3 μm confirms the conclusion that the scaling between [CII] and PAH is independent of source classification. The correlation of [CII] with a SFR indicator can be checked in a completely independent way using the comparison between [CII] with [NeII], because [NeII] is a luminosity indicator of star formation determined by the HII region instead of the surrounding PDR. Another comparison between the [CII]/[NeII] ratio and the classification shows a result very similar to the [CII]/PAH comparison. The median ratios f([CII])/f([NeII]) are independent of classification. The dispersion about the median is also similar to the dispersion in [CII]/PAH. Because [NeII] arises primarily from SBs, this result is very important empirically because it confirms the previous conclusion from PAH that [CII] scales with the SB component within sources of all classifications

implying that the SB component and SFR is measured equally well by PAH emission or by [CII] emission in sources of all classifications.

5. *Neon lines comparison to [CII] 158 μm line:*
   We obtain that [CII] and [NeII] perfectly scale with one another and represent the SB component of the galaxy. However, there is a greater difference of ratio with classification than for [NeII]. The increasing ratio f([CII])/f([NeIII]) from AGNs to SBs can be explained if [NeIII] arises both from AGN ionization and SB ionization, but [CII] arises only from SBs, so that AGNs contain an additional [NeIII] component compared to [CII].
6. *Classification of [CII] 158 μm line profiles:*
   I have classified all of the [CII] profiles by shape (Gaussian, asymmetric and flattened), as compared to the best fitted Gaussian profiles illustrated in http://cassis.sirtf.com/herschel. The objective of this classification is to distinguish among profiles obviously affected by disk rotation and those profiles which probably arise because of virialized three dimensional motions of the gas. Flattened profiles are those which have the clearest evidence of velocities dominated by rotation. Asymmetric profiles show evidence either of systematic gas outflows, or of rotation by an inhomogeneous disk.
7. *[CII] 158 μm line profiles compared to different luminosities:*
   [CII] emission line widths are compared to [CII] luminosities, to near-infrared 1.6 μm (H) luminosities and to infrared 22 μm luminosities to decide if any luminosity accurately relates to velocity dispersion. The luminosity dispersions are smallest for H band luminosities and the slope uncertainty for the line fit is the smallest for H luminosities. I conclude that the gravity associated with the mass of evolved stars (H luminosities) is a weak factor controlling the widths of the [CII] line, but line widths are primarily determined by a mechanism that is still unknown.

Overall, this thesis provides significant advancements in the methodologies used to study dusty galaxies and AGN, bridging gaps in our knowledge of galaxy evolution across cosmic time. Together, these results demonstrate the immense importance of studying infrared data in understanding fundamental evolutionary processes in galaxies. The detailed calibrations, classification methods, and redshift correction methods introduced in this work provide a foundation for future studies of the distant Universe.

Approbation of the work

The results of the thesis were presented at the following conferences:

1. The Third Middle-East and Africa Regional IAU meeting, September 1-6, 2014, Beirut, Lebanon
2. Astronomical Surveys and Big Data, October 5-8, 2015, Byurakan, Armenia
3. Armenian - Iranian astronomical workshop, October 13-16, 2015, Byurakan, Armenia
4. Non-Stable Universe: Energetic Resources, Activity Phenomena and Evolutionary Processes, September 19-23, 2016, Byurakan, Armenia
5. European Week of Astronomy and Spasce Science 2017: EWASS2017, 26 – 30 June, 2017, Prague, Czech Republic
6. Stellar Associations: 70 Years of Research/The Present and Future of Small and Medium Telescopes, September 25-29, 2017, Byurakan, Armenia
7. VII Pulkovo young scientists conference, Pulkovo Observatory, 28-31 May, 2018, Saint Petersburg, Russia
8. Instability Phenomena and Evolution of Universe, September 17-21, 2018, Byurakan, Armenia
9. First Light: Stars, galaxies and black holes in the epoch of reionization, Jul. 28 - Aug. 7, 2019, Sao Paulo, Brazil
10. "4th SVOSS (Super Vatican Observatory Summer School)" conference, Sept. 3-7, 2019, Vatican, Italy
11. European Astronomical Society Annual Meeting (EAS) 2022, June 27- July 1, 2022, Valencia, Spain
12. European Astronomical Society Annual Meeting (EAS) 2023, July 10-14, 2023, Krakow, Poland
13. Non-Stable Phenomena in the Universe, September 18-21, 2023, Byurakan, Armenia

Structure of the thesis

The thesis consists of 6 chapters including Introduction and main Conlusions. In addition, there are separate sections for Acknowledgements and References. The thesis contains 123 pages, including two title pages in Armenian and in English.

Content of the thesis

Chapter 1

This chapter introduces infrared astronomy as a critical tool for studying active galaxies, with a particular focus on the [CII] 158 μm emission line. It outlines how infrared radiation penetrates dust clouds, enabling the study of star formation and galactic nuclei obscured in other wavelengths. The [CII] line, arising from photodissociation regions (PDRs), provides insights into star formation rates (SFR) and interstellar medium (ISM) properties. Viktor Ambartsumian's foundational contributions to understanding active galactic nuclei (AGN) are highlighted, emphasizing the dynamic and energetic processes in galactic cores. The chapter sets the stage by identifying the importance of [CII] as a diagnostic tool and describes the challenge of disentangling AGN-driven and starburst-driven processes in dusty environments.

Understanding the initial formation of galaxies depends on discovering sources obscured by dust and tracing these sources to their earliest epoch in the universe. The extreme luminosity of dusty, local sources was originally revealed by the ultraluminous infrared galaxies (ULIRGs), whose luminosity arises from infrared emission by dust, and this dust often obscures the primary optical sources of luminosity. That such galaxies are important in the early universe was demonstrated by source modeling which indicated that the infrared dust emission from galaxies dominates the cosmic background.

Surveys in the submillimeter were the first to discover individual, optically obscured, dusty sources at redshifts $z >= 2$. A variety of observing programs using spectra from the Spitzer Infrared Spectrometer (IRS) subsequently found luminous ULIRGs to redshifts $z\sim3$. This Spitzer-discovered population of high-redshift ULIRGs has large infrared-to-optical flux ratios [fv (24 μm) > 1 mJy and R > 24] attributed to heavy extinction by dust and has been labeled "dust obscured galaxies" (DOGs). Some DOGs are powered primarily by starbursts and some by active galactic nuclei (AGNs), and the DOGs are similar to the population of submillimeter galaxies in overall spectral energy distributions (SEDs), redshifts, and Luminosities.

To discover and understand dusty galaxies at even higher redshifts than the DOGs known so far, the atomic line emission of [CII] 158 μm is the single most important spectroscopic feature because it is the strongest far-infrared line. Consequently, this line will provide the best opportunity for redshift determinations and source diagnostics using submillimeter and millimeter spectroscopic observations. Already, [CII] has been detected at redshift exceeding 7 and shown to be strong in starbursts with $1 < z < 2$. The [CII] line should be a diagnostic of star formation because it is primarily associated with the photodissociation region (PDR) surrounding starbursts (SBs).

In many high-redshift sources, especially dust-obscured sources, the [CII] feature is the only diagnostic atomic emission line that can be observed. This makes it vital to optimize this line for learning about intrinsic source properties. Not only line luminosities, but also accurate line profiles, are observed.

A great amount of diagnostic information concerning the observable differences between dusty, obscured sources powered by active galactic nuclei (AGNs) and those powered by rapid star formation ("starbursts") has been acquired via the mid-infrared spectroscopy of the Infrared Spectrograph (IRS) on the Spitzer Space Telescope. Classifications of AGN and starburst sources have been developed using both the strength of polycyclic aromatic hydrocarbon (PAH) features in low-resolution spectra and various emission line ratios in high-resolution spectra.

These findings underscore the critical role of far-infrared diagnostics, particularly the [CII] 158 μm emission line, in unraveling the complexities of galaxy evolution. The integration of mid-infrared spectroscopic tools, submillimeter observations, and advanced classifications has significantly advanced our ability to differentiate between AGN-driven and starburst-driven processes in dusty, high-redshift galaxies. By leveraging the [CII] line as a robust tracer of star formation and interstellar medium properties, this research provides a foundation for probing the earliest stages of galaxy formation, bridging observational gaps, and refining models of cosmic evolution. The capability to study both the physical conditions and kinematics of these distant galaxies sets a path for future explorations, further enabling the discovery of hidden populations of galaxies in the early universe.

Chapter 2

This chapter presents observational data from the Herschel Space Observatory, detailing [CII] measurements in 112 sources classified as AGNs, Starbursts, or Composites. A strong correlation is observed between [CII] luminosity and PAH (Polycyclic Aromatic Hydrocarbon) emission, affirming [CII] as a reliable tracer of star formation in photodissociation regions. The calibration of SFR with [CII] luminosity is introduced, yielding a robust relation for dusty galaxies. The "[CII] deficit" in luminous AGNs is analyzed, suggesting that AGN dominance reduces [CII] emission relative to total infrared luminosity. The chapter underscores the significance of [CII] as a tool for probing dusty galaxies at high redshifts.

The Herschel PACS instrument has been used to observe [CII] 158 μm line fluxes in 112 sources having a wide range of starburst and AGN classifications chosen because they

have complete mid-infrared spectra with the Spitzer IRS and have complete IRAS fluxes for determining L_{ir}. Of the 112 sources, 102 have reliable line detections and 10 are upper limits.

It is found that the [CII] line flux correlates with the flux of the 11.3 μm PAH feature, log [f([CII] 158 μm)/f(11.3 μm PAH)] = −0.22 ± 0.25. This f([CII])/f(PAH) ratio is independent of AGN/starburst classification as determined from EW of the 6.2 μm PAH feature. We conclude that [CII] line flux measures the starburst component of any source as reliably as the PAH feature.

This conclusion leads to a calibration of SFR determined from the luminosity of [CII] for the Starburst component in any source. The calibration is derived using L_{ir} only for starbursts to avoid AGN contamination of L_{ir} and has the result log SFR = log L([CII]) − 7.08 ± 0.3, for SFR in $M_\odot$ yr^{-1} and L([CII]) in $L_\odot$. This result applies to the starburst component of any source in which [CII] is observed. The maximum SFRs in the sample are 100 $M_\odot$ yr^{-1}, and SFRs are dominated by sources classified as Starbursts, but most AGNs also have some measurable Starburst component.

The [CII] "deficit," or a smaller ratio of L([CII])/L_{ir} with increasing L_{ir}, is shown to arise because L_{ir} of the most luminous sources arises primarily from an AGN so that L([CII]) from the Starburst component is small in comparison.

Chapter 3

This chapter explores the relationship between [CII] and mid-infrared emission lines, including neon lines, to enhance SFR diagnostics. Observations from the Spitzer IRS and Herschel PACS instruments are used to compare [CII] flux with mid-infrared continuum and emission features. The chapter discusses the ratio of [CII] luminosity to mid-infrared continuum luminosities as a diagnostic of star formation and AGN activity. Key findings include the calibration of SFR using [CII] and neon lines, highlighting their complementary roles in disentangling Starburst and AGN contributions.

Results for 112 sources are compared with emission line fluxes from high resolution Spitzer IRS spectra. A new calibration of [CII] as an SFR indicator is determined by comparing [CII] fluxes with mid-infrared [NeII] and [NeIII] emission line fluxes. This independently gives the same result as determining SFR using bolometric luminosities of reradiating dust from SBs: log SFR = log L ([CII]) − 7.0 ± 0.2, for SFR in $M_\odot$ yr^{-1} and L ([CII]) in $L_\odot$. This confirms that [CII] measures the same SB component of sources as measured with mid-infrared PAH and neon emission line diagnostics.

The line to continuum ratio measured at 158 μm, EW ([CII]), changes little with luminosity or with classification, indicating that the far-infrared continuum at 158 μm arises primarily from the SB component of any source. For pure SBs, the continuum alone gives log SFR = log νL_ν (158 μm) – 42.8 ± 0.2 for SFR in $M_\odot$ yr^{-1} and νL_ν (158 μm) in erg s^{-1}. The change of EW ([CII]) with classification (median EW ([CII]) = 1.0 μm for SBs compared to 0.7 μm for AGNs) implies a systematic overestimate of SFR in AGNs by a median factor of 1.4 if using only the far-infrared continuum at 158 μm as an SFR indicator.

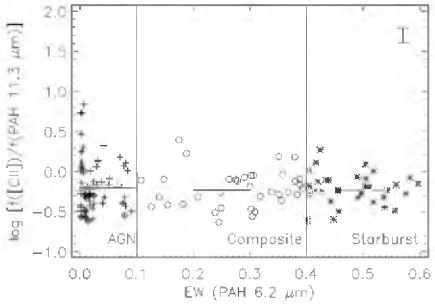

Fig 3-1. Ratio of [C II] 158μm to PAH 11.3μm line fluxes, compared to the source classification from EW(PAH 6.2μm)

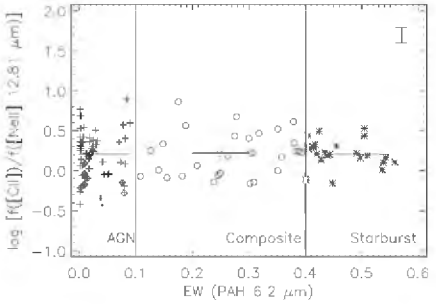

Fig 3-2. Ratio of [C II] 158μm to [Ne II] 12.81μm line fluxes, compared to source classification from EW(PAH 6.2μm)

The comparison with PAH in Figure 3-1 confirms, that the scaling between [C II] and PAH is independent of source classification, implying that the SB component and SFR is measured equally well by PAH emission or by [C II] emission in sources of all classifications. The correlation of [C II] with an SFR indicator can be checked in a completely independent way using Figure 3-2, which compares [C II] with [Ne II], because [Ne II] is a luminosity indicator of star formation determined by the HII region instead of the surrounding PDR.

Chapter 4

The focus shifts to the analysis of [CII] and neon emission line profiles, examining their widths and velocities. High-resolution spectra from Herschel PACS and Spitzer IRS are used to compare line profiles across AGN and Starburst-dominated sources. Differences in line widths and radial velocities provide insights into the kinematic properties of gas in different environments. The chapter concludes that [CII] and neon lines offer complementary kinematic diagnostics, revealing the dynamics of star-forming regions.

We measure emission line profiles and redshifts for extragalactic sources observed in both [CII] 158 μm with Herschel PACS and in [NeII] 12.81 μm and [NeIII] 15.55 μm with the high-resolution Spitzer IRS. Data are presented and compared for 379 different sources. Results for [CII] and neon are compared by locating the PACS observing spaxel that most closely corresponds to the position of the IRS slit. Intrinsic line profile widths are determined by applying empirically measured instrumental widths from observed planetary nebulae or HII regions. All [CII] and neon line profiles, together with overlays of PACS spaxels compared to IRS slits, are illustrated in the CASSIS spectral atlas (*http://cassis.sirtf.com/herschel*). Figure 4-1 represents an example of the overlay of Herschel PACS spaxels and Spitzer IRS high-resolution slits.

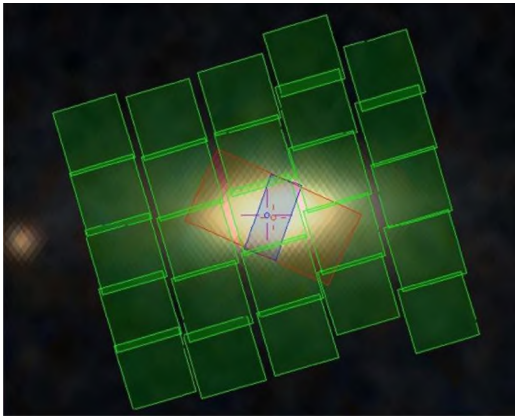

Fig. 4-1. Example of PACS spaxels compared to IRS high-resolution slits, for source Markarian 18.

Sources are classified as AGNs, Composites, or Starbursts based on the equivalent width of the PAH 6.2 μm feature.

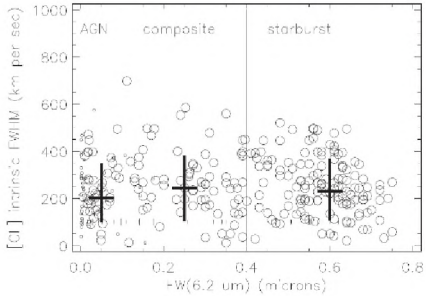

Fig. 4-2. Intrinsic FWHM of [C II] 158 μm" in km s–1 compared to EW(6.2 μm)

The median intrinsic FWHM for [CII] shows no change with classification, being 207 km s^{-1} for AGNs, 248 km s^{-1} for Composites, and 233 km s^{-1} for Starbursts with dispersions in intrinsic line widths of about ±130 km s^{-1}. Results show that [CII] line widths generally match those of [NeII], as previously indicated in comparisons of line fluxes. A small number of sources are identified with unusually broad lines or with radial velocity differences between [CII] and neon measures. Accurate redshifts are determined for sources as demonstrated by a systematic difference of only 21 km s^{-1} between the independent measures of [CII] and [NeII] radial velocities using PACS and IRS.

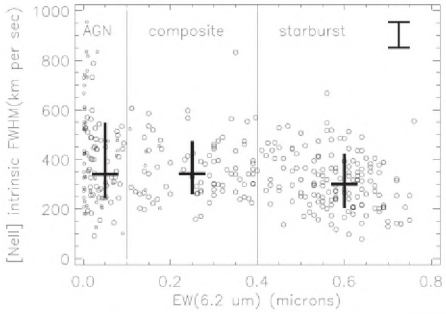

Fig. 4-3. Intrinsic FWHM of [Ne II] 12.81 μm in km s^{-1} compared to EW(6.2 μm)

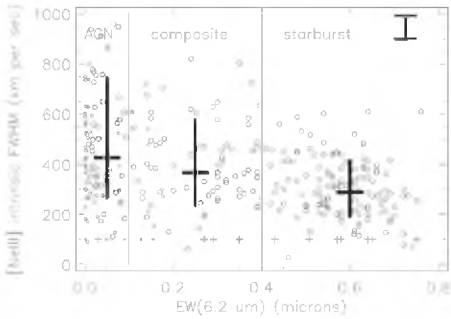

Fig. 4-4. Intrinsic FWHM of [Ne III] 15.55 μm in km s^{-1} compared to EW(6.2 μm)

The results for [Ne II] in Figure 4-3 show a similar result to [C II], with only a slight trend of increased widths for AGNs; the median FWHM for AGNs and composites is 340 km s^{-1} compared to 300 km s^{-1} for starbursts. The best comparison with [C II] is for the starbursts to rule out any broadening of [Ne II] by an AGN. For starbursts, the difference between the median FWHM of 233 km s^{-1} for [C II] and 300 km s^{-1} for [Ne II] is interesting, but we cannot be confident that it is meaningful. Despite these uncertainties among comparisons of [C II] and neon line widths, the relative widths between the [Ne II] and [Ne III] lines are meaningful. Unlike the [Ne II] FWHMs in Figure 4-3, the [Ne III] FWHMs in Figure 4-4 show a trend for increasing line widths from starbursts through AGNs. Both the median values of line widths and the upper values of the dispersions are progressively larger from starbursts through composites to AGNs, with medians of 289 km s^{-1} for starbursts, 367 km s^{-1} for composites, and 426 km s^{-1} for AGNs.

Chapter 5

This chapter provides a detailed analysis of [CII] line widths, focusing on their implications for gas dynamics in dusty galaxies. The sample includes sources where [CII] profiles reveal variations in turbulence and ionization. The chapter discusses the interplay between AGN-driven outflows and Starburst-driven winds, emphasizing the role of [CII] as a kinematic tracer. Findings suggest that line width variations correlate with galaxy type and luminosity, offering clues about the energy sources shaping galaxy evolution.

I classify [CII] 158 μm profiles for 379 galaxies observed with Herschel PACS as Gaussian, flattened and asymmetric based on the comparison of observed profiles to Gaussian fits.

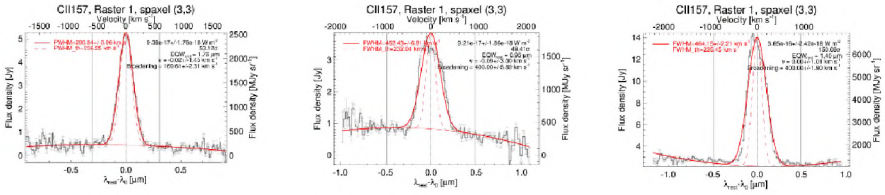

Fig. 5-1. Examples of profile classifications as Gaussian (left, NGC3393), flattened (central, NGC7603) and asymmetric (right, ESO323-G077)

Profile shapes in Figure 5-1 can indicate the origin of the line widths because the lines whose width is caused by three dimensional random motions in a galaxy should be Gaussian, but widths caused by rotation of a disk should not be Gaussian. Emission line widths are compared to [CII] luminosities (which scales primarily with the photodissociation regions surrounding starbursts and so scales with the gas mass connected to star formation), to near-infrared 1.6 μm luminosities (which scales with the total luminosity of the evolved stars) and to infrared 22 μm luminosities (which scales with the total luminosity of younger, hotter stars that are heating the dust) to decide if any luminosity accurately relates to velocity dispersion. The fits in Figure 5-2 are shown using linear values for FWHM to compare scatter among the comparisons using the different parameters. These plots show the scatter in the luminosity distributions above and below the formal fits (± 1σ for log L) within three different ranges of FWHM. In all cases, the scatter is extreme. The range of luminosities at a given value of FWHM is comparable in all cases to the full range of FWHM over all luminosities. There can be a factor of 5 range in gas velocities for the same value of luminosity. It does not appear, therefore, that FWHM for [CII] can be used in a meaningful way to predict any kind of galaxy luminosity.

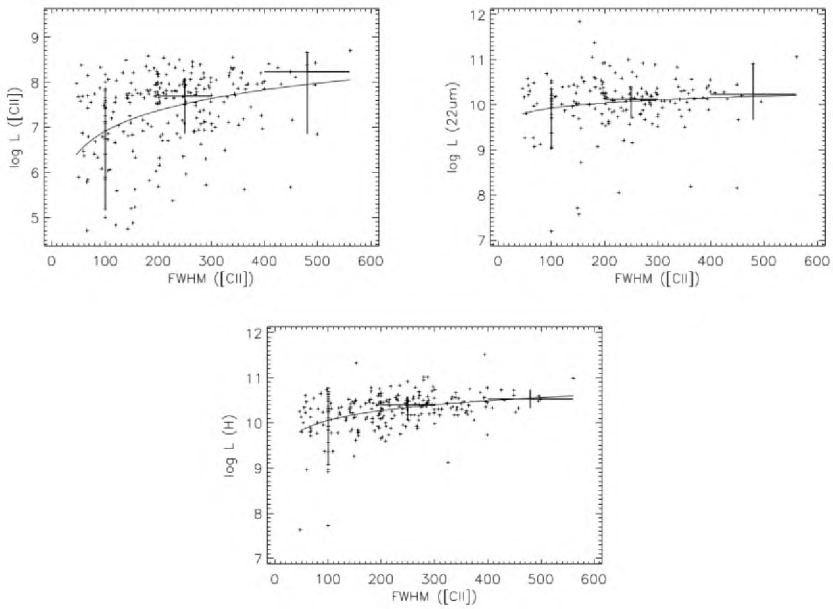

Fig. 5-2. Luminosities compared to FWHM (linear scale). Vertical lines show 1σ dispersions for velocities 100 km sec^{-1}, 200-300 km sec^{-1} and >400 km sec^{-1}.

The luminosity dispersions are smallest for H band luminosities and the slope uncertainty for the line fit is the smallest for H luminosities. I conclude from this that the gravity associated with the mass of evolved stars is a weak factor controlling the widths of the [CII] line, but line widths are primarily determined by a mechanism that is still unknown.

Chapter 6

The final chapter summarizes the thesis findings, emphasizing the pivotal role of the [CII] 158 μm line in studying dusty Starburst galaxies and AGNs. It reaffirms [CII] as a robust tracer of star formation and ISM conditions, even in high-redshift and obscured environments. The integration of [CII] with mid-infrared diagnostics provides a comprehensive framework for disentangling AGN and Starburst contributions. The conclusions highlight the importance of [CII] for future studies of galaxy evolution, particularly in the early universe, where it remains a key diagnostic tool for uncovering obscured star formation and black hole activity.

This comprehensive study used Herschel PACS observations of the [CII] 158 μm fine-structure line, combined with Spitzer IRS mid-infrared spectroscopy and IRAS fluxes, to investigate the properties of a large sample of galaxies spanning a broad range of star

formation and active galactic nucleus (AGN) activity. The results firmly establish [CII] as a robust tracer of the star-forming (Starburst) component in galaxies and provide valuable calibrations and insights into star formation rates, kinematics, and the interplay of AGNs and Starbursts.

Across the sample, [CII] emission correlates strongly with mid-infrared polycyclic aromatic hydrocarbon (PAH) features, notably the 6.2 μm and 11.3 μm PAH lines, and with mid-infrared [NeII] line, which means that both [CII] and [NeII] represent the Starburst component of the galaxy. The consistency of these relationships, independent of whether a source is dominated by star formation or an AGN, demonstrates that [CII] measures the Starburst component as reliably as established mid-infrared tracers. The result is a firm calibration of star formation rates (SFRs) from [CII] luminosity:

$$\text{Log (SFR)} = \log (L\,[\text{CII}]) - 7.0 \pm 0.2,$$

where SFR is in $M_\odot\ yr^{-1}$ and L([CII]) in $L_\odot$. This relation applies not just to pure Starburst galaxies but also to systems where AGNs are present, allowing isolation of the star-forming contribution even in Composite sources.

While the [CII]/IR ratio generally declines at the highest infrared luminosities—known as the [CII] "deficit", these findings clarify that this phenomenon arises primarily because luminous sources often have a substantial AGN component inflating their total infrared output. Consequently, the proportion of [CII] coming from star formation ap-pears smaller against the AGN-driven IR continuum. When the Starburst component is isolated, [CII] remains a faithful measure of the star formation activity.

The ratio of [CII] line flux to the continuum at 158 μm remains relatively constant across classifications, suggesting that the far-infrared continuum near 158 μm is also domi-nated by star-forming regions. For pure Starbursts, the continuum alone at 158 μm provides a secondary SFR indicator. However, in AGN-dominated systems, using only the far-infrared continuum to estimate SFR can lead to moderate overestimates (by a factor of about 1.4). This highlights the importance of line diagnostics like [CII] for ac-curate SFR estimates in complex systems.

High-resolution measurements of [CII] line profiles and comparisons with neon lines reveal that line widths and kinematics are broadly similar across AGN, Composite, and Starburst classifications. The median intrinsic [CII] line widths (~200–250 km s^{-1}) do not depend strongly on nuclear activity type. Moreover, [CII] and [NeII] lines yield con-sistent redshifts, demonstrating the utility of these far-infrared and mid-infrared lines as reliable probes of galaxy velocities and distances.

Analysis of [CII] line profiles show a range of shapes—Gaussian, flattened, or asymmetric—implying that not all linewidths are driven purely by random motions. While comparing line widths to various luminosities suggests that the gravitational potential traced by the mass of more evolved stars (as indicated by H-band luminosity) may modestly influence the observed kinematics, the dominant mechanism controlling [CII] line width remains unclear.

These results solidify the role of [CII] 158 μm emission as a key diagnostic of star formation in diverse galactic environments. They demonstrate that [CII] emission is an integral counterpart to mid-infrared emission line and PAH diagnostics, providing robust SFR measures and aiding in disentangling star formation from AGN effects. In addition, the kinematic analyses improve our understanding of the gas dynamics in galaxies, though further work is needed to pinpoint the main drivers of the observed velocity dispersions.

In summary, [CII] emerges as a powerful, versatile tool for studying the star-forming properties and kinematics of galaxies, serving as a cornerstone for multi-wavelength analyses of galaxy evolution.

Publications in the topic of the thesis

1. Sargsyan, L. ; Lebouteiller, V. ; Weedman, D. ; Spoon, H. ; Bernard-Salas, J. ; Engels, D. ; Stacey, G. ; Houck, J. ; Barry, D. ; Miles, J. ; **Samsonyan, A.** ; [C II] 158 μm Luminosities and Star Formation Rate in Dusty Starbursts and Active Galactic Nuclei ; The Astrophysical Journal, Volume 755, Issue 2, article id. 171, 13 pp. (2012).

2. Sargsyan, L. ; **Samsonyan, A.** ; Lebouteiller, V. ; Weedman, D. ; Barry, D. ; Bernard-Salas, J. ; Houck, J. ; Spoon, H. ; Star Formation Rates from [C II] 158 μm and Mid-infrared Emission Lines for Starbursts and Active Galactic Nuclei ; The Astrophysical Journal, Volume 790, Issue 1, article id. 15, 12 pp. (2014).

3. **Samsonyan, Anahit** ; Weedman, Daniel ; Lebouteiller, Vianney ; Barry, Donald ; Sargsyan, Lusine ; Neon and [C II] 158 μm Emission Line Profiles in Dusty Starbursts and Active Galactic Nuclei ; The Astrophysical Journal Supplement Series, Volume 226, Issue 1, article id. 11, 18 pp. (2016).

4. **Samsonyan, A. L.** ; Analysis of Emission Line Widths of [CII] 158μm ; Astrophysics, Volume 65, Issue 2, pp. 151-160 (2022)

Ամփոփագիր

Ատենախոսության հիմնական նպատակն է ուսումնասիրել ֆիզիկական հատկությունները և պրոցեսները, որոնք տեղի են ունենում փոշով հարուստ աստղառաջացման բռնկումով գալակտիկաներում (Starburst galaxies - SB) և ակտիվ գալակտիկական միջուկներում (ԱԳՄ, Active Galactic Nuclei -AGN)՝ օգտագործելով [CII] 158 մկմ առաքման գիծը որպես հիմնական վերլուծական գործիք:
Ուսումնասիրելով [CII] լուսատվությունների, աստղառաջացման տեմպի (Star Formation Rate - SFR), ինչպես նաև՝ միջին-ենթակարմիր առաքման գծերի միջև կապը՝ հետազոտությունը նպատակ ունի. ուսումնասիրել գալակտիկաներում աստղառաջացման և գալակտիկայի միջուկի ակտիվության միջև կապը, սահմանել [CII] 158 մկմ առաքման գիծը՝ որպես աստղառաջացման տեմպի բնութագիր, հատկապես՝ փոշով հարուստ միջավայրերում, ստանալ պատկերացումներ գալակտիկաների էվոլյուցիոն փուլերի մասին՝ կենտրոնանալով հատկապես մեծ կարմիր շեղում ունեցող փոշով կլանված հեռավոր համակարգերի վրա:
Այս աշխատանքը նպաստում է ենթակարմիր առաքման գծերի դերը գալակտիկաների առաջացման շարժիչ պրոցեսներում հասկանալու և այդ պրոցեսները դեպի էվոլյուցիոն ավելի վաղ փուլեր մոդելավորելուն:
Ատենախոսության հիմնական արդյունքներն են.

1. *379 ակտիվ գալակտիկաների դասակարգումը.*
   Մենք դասակարգել ենք 379 ակտիվ գալակտիկաներ ԱԳՄ-ների, բաղադրյալ աղբյուրների և աստղառաջացման բռնկումով գալակտիկաների, որոնք դիտվել են և՛ Սպիցերի տիեզերական աստղադիտակով, և՛ Հերշելի տիեզերական աստղադիտարանով: Արդյունքները ստացվել են՝ հաշվի առնելով Հերշելի դիտված «սպեքսըլ»-ի (Herschel observed spaxel) և Սպիցերի դիտված ճեղքի (Spitzer IRS observed slit) դիրքերը: Բոլոր [CII] և նեոնի ([NeII] և [NeIII]) պրոֆիլները, ինչպես նաև՝ Հերշելի «սպեքսըլ»-ի և Սպիցերի ճեղքի վերադրումները, ներկայացված են Սպիցերի սպեկտրերի CASSIS (Combined Atlas of Sources with Spitzer IRS Spectra) արխիվում (http://cassis.sirtf.com/herschel):
2. *Աստղառաջացման տեմպի (SFR: star formation rate) տրամաչափում.*
   Աշխատանքը տրամադրում է աստղառաջացման տեմպի հստակ տրամաչափում, մասնավորապես՝ փոշով հարուստ միջավայրերում, որտեղ մինչ այժմ մեզ հայտնի օպտիկական գծերը, որոնք չափում էին աստղառաջացման տեմպը, կլանվում են: Ատենախոսությունը [CII] լուսատվության և աստղառաջացման տեմպի համար տալիս է հետևյալ գնահատականը. $\log(SFR) = \log L([CII]) - 7.0 \pm 0.2$ (աստղառաջացման տեմպը $M_\odot$ տարի$^{-1}$ և $L([CII])$-ն $L_\odot$ միավորներով):
3. *6.2 մկմ ՊԱՀ-ը (Polycyclic Aromatic Hydrocarbon - PAH) որպես դասակարման միջոց.*

Գալակտիկաների դասակարգման համար մենք որդեգրել ենք հետևյալ չափանիշը. եթե գծի EW (էկվիվալենտ լայնությունը)՝ EW (6.2 μm) < 0.1 μm, այս աղբյուրները դասակարգվել են որպես ԱԳՄ-ներ, եթե 0.1 μm < EW (6.2 μm) < 0.4 μm, ապա՝ միջանկյալ աղբյուրներ, իսկ եթե EW (6.2 μm) > 0.4 μm, դասակարգվել են որպես աստղառաջացման բռնկումով գալակտիկներ:

4. *[CII] 158 մկմ գիծը որպես աստղառաջացման բնութագիր.*
   Տարբեր բնութագրերի համեմատման արդյունքում ստացվել է, որ [CII] 158 մկմ գծի հատկանիշները անփոփոխ են մնում տարբեր դասակարգումների դեպքում և չեն փոփոխվում ԱԳՄ-ի առկայության դեպքում, հետևաբար՝ հստակ կարելի է այն համարել որպես աստղառաջացման ցուցիչ:
5. *Նեոնի գծերի համեմատությունը [CII] 158 մկմ գծի հետ.*
   Ստացել ենք, որ, ինչպես [CII] 158 մկմ-ը, այնպես էլ՝ [NeII] 12.81 մկմ-ը, բնութագրում են գալակտիկայի աստղառաջացնող կոմպոնենտը, մինչդեռ՝ [NeIII] 15.55 մկմ գիծը ունի կոմպոնենտ՝ ազդված ԱԳՄ-ի կողմից:
6. *[CII] 158 մկմ գծի պրոֆիլների դասակարգումը.*
   Գծի պրոֆիլները դասակարգվել են գաուսիան, ասիմետրիկ և հարթեցված տիպերի, որի նպատակն է տարբերակել այն պրոֆիլները, որոնք ակհայտորեն ազդված են գալակտիկայի սկավառակի պտույտից (հարթեցված) և որոնք հավանաբար առաջանում են գազի եռաչափ շարժման հետևանքով (ասիմետրիկ):
7. *[CII] 158 մկմ գծի պրոֆիլների համեմատությունը տարբեր լուսատվությունների հետ.*
   [CII] առաքման գծի կիսալայնությունները համեմատել ենք իր իսկ լուսատվությունների հետ (բնութագրում է աստղառաջացման հետ կապված գազի զանգվածը), մոտ-ենթակարմիր (H 1.6 մկմ) (բնութագրում է ավելի զարգացած ոչ երիտասարդ աստղերի լուսատվությունը) և ենթակարմիր 22 մկմ (բնութագրում է ավելի երիտասարդ, ջերմ աստղերի լուսատվությունը, որոնք տաքացնում են փոշին) լուսատվությունների հետ՝ որոշելու համար՝ արդյոք [CII] արագությունները կապված են գալակտիկայի որևէ լուսատվության հետ: Ստացվել է՝ լուսատվության ցրումները, ինչպես նաև՝ թեքի սխալները ամենափոքրն են H լուսատվության համար, որից կարող ենք եզրակացնել, որ ավելի կազմավորված աստղերի զանգվածը կարող է հանդիսանալ [CII]-ի լայնությունների վերահսկման թույլ գործոն:

Автореферат

Основная цель этой диссертации - исследовать физические свойства и процессы, происходящие в галактиках со вспышкой звездообразования и активных ядрах галактик (АЯГ: AGN), богатых пылью, используя линию излучения [CII] 158 мкм в качестве диагностического инструмента. Изучая корреляцию между светимостями в линии [CII], скоростями звездообразования (SFR) и особенностями излучения в среднем инфракрасном диапазоне, исследование направлено на: улучшение понимания взаимодействия между звездообразованием и активностью AGN в галактиках, усовершенствование использования линии [CII] 158 мкм в качестве надежного индикатора для SFR, особенно в богатых пылью средах, обеспечение понимания эволюционных фаз развития галактик, сосредоточившись на системах с высоким красным смещением, скрытых пылью.

Эта работа вносит вклад в более широкие усилия по пониманию роли линий инфракрасного излучения в отслеживании процессов, управляющих формированием и эволюцией галактик на протяжении хабловского времени.

Основными результатами диссертации являются:

1. Классификация 379 галактик:
   Мы классифицируем 379 галактики как AGN, Composite или Starburst, наблюдавшиеся как с помощью космического телескопа Спитцер, так и с помощью космической обсерватории Гершель. Результаты для [CII] и линий неона [NeII], [NeIII] сравниваются путем определения местоположения наблюдательного спекселя PACS (PACS spaxel), который наиболее точно соответствует положению щели IRS. Собственные ширины профилей линий определяются путем применения эмпирических измеренных инструментальных ширин из наблюдаемых планетарных туманностей или областей HII. Все профили линий [CII] и неона вместе с наложениями спекселей PACS по сравнению со щелями IRS проиллюстрированы в спектральном атласе CASSIS (*http://cassis.sirtf.com/herschel*).
2. Калибровка скорости звездообразования (SFR) с использованием эмиссионной линии [CII] 158 мкм:
   Работа обеспечивает стабильную калибровку скорости звездообразования, особенно в пылевых средах, где известные оптические линии, измеряющие скорость звездообразования, поглощаются. В диссертации показано, что светимость [CII] в некоторой степени зависит от скорости звездообразования следующим образом: $\log(SFR) = \log L([CII]) - 7{,}0 \pm 0{,}2$ для SFR в $M_\odot$ год$^{-1}$ и L([CII]) в $L_\odot$.
3. Характеристика 6,2 мкм ПАУ как критерий классификации:
   Мы приняли критерии, что АЯГ имеют EW (6,2 мкм) < 0,1 мкм, составные источники имеют промежуточные 0,1 мкм < EW (6,2 мкм) < 0,4 мкм, а галактики со вспышечным звездообразованием имеют EW (6,2 мкм) > 0,4

мкм. Этот критерий классификации обеспечивает надежный метод для выявления основных движущих сил галактического излучения рассматриваемых обьектов.

4. [CII] 158 мкм линия как индикатор звездообразования:
   В результате сравнения различных характеристик было установлено, что особенности линии [CII] 158 мкм остаются неизменными при разных классификациях и не изменяются в присутствии АЯГ, поэтому ее однозначно можно рассматривать как индикатор звездообразования.
5. Сравнение линий неона с линией [CII] 158 мкм:
   Показано, что как [CII] 158 мкм, так и [NeII] 12,81 мкм характеризуют звездообразующий компонент галактики, в то время как линия [NeIII] 15,55 мкм обусловлена компонентом среды, на который влияет АЯГ.
6. Классификация профилей линий [CII] 158 мкм:
   Я классифицировала все профили [CII] по форме (гауссовы, асимметричные и сплющенные). Цель этой классификации — различить профили, явно затронутые вращением диска (сплющенные), и те профили, которые, вероятно, возникают из-за вириализованных трехмерных движений газа (асимметричные).
7. Сравнение профилей линии [CII] 158 мкм с различной светимостью:
   Ширина эмиссионной линии [CII] сравнивается со светимостью в линии [CII] 158 мкм (характеризует массу газа, связанного с образованием звезд), со светимостью в ближнем инфракрасном диапазоне 1,6 мкм (H) (характеризует светимость более развитых, старых звезд) и со светимостью в инфракрасном диапазоне 22 мкм (характеризует светимость молодых, более горячих звезд, которые нагревают пыль), чтобы выявить, связана ли какая-либо светимость с дисперсией скорости. Дисперсии светимости наименьшие для светимости в полосе H, а неопределенность наклона для подгонки линии наименьшая для светимости в полосе H. Я прихожу к выводу, что гравитация, связанная с массой эволюционировавших звезд (светимостью H), является слабым фактором, контролирующим ширину линии [CII], но ширина линии в первую очередь определяется механизмом, который до сих пор неизвестен.

Անահիտ Սամսոնյան / Anahit Samsonyan / Анаит Самсонян _____